Advances in Molten Slags, Fluxes, and Salts: Proceedings of The 10th International Conference on Molten Slags, Fluxes and Salts (MOLTEN16)
Edited by: Ramana G. Reddy, Pinakin Chaubal, P. Chris Pistorius, and Uday Pal
TMS (The Minerals, Metals & Materials Society), 2016

EQUILIBRIA OF GOLD AND SILVER BETWEEN MOLTEN COPPER AND FeO_X-SiO_2-Al_2O_3 SLAG IN WEEE SMELTING AT 1300 °C

Katri Avarmaa[1], Hugh O'Brien[2], Pekka Taskinen[1]

[1]Aalto University School of Chemical Technology, Department of Materials Science and Engineering, Metallurgical Thermodynamics and Modeling Research Group;
Vuorimiehentie 2K, PO Box 16200, FI-00076 Aalto, Finland
[2]Geological Survey of Finland;
Betonimiehenkuja 4, 02150 Espoo, Finland.

Keywords: Distribution, Precious metal, Copper smelting, E-scrap, EPMA, LA-ICP-MS

Abstract

Waste Electrical and Electronic Equipment (WEEE) offers a significant resource for precious metals such as gold and silver. To maximize precious metal recoveries and sustainable use their behavior during WEEE smelting with copper as the collector metal needs to be characterized. This study experimentally determines the distributions of gold and silver between metallic copper and FeO_x-SiO_2-Al_2O_3 slag ($L^{Cu/s}[Me] = [Me]_{Copper}/[Me]_{Slag}$) in alumina-saturation over the oxygen potential range of 10^{-5}–10^{-10} atm at 1300 °C. The experiments were conducted employing equilibration / quenching followed by major element analysis by Electron Probe Micro-Analysis (EPMA) and trace element analysis by Laser Ablation Inductively Coupled Mass Spectrometry (LA-ICP-MS) techniques. Our results show silver distribution increased exponentially from 30 to 1000 as a function of decreasing oxygen partial pressure. Gold distribution was 10^5 at $pO_2 = 10^{-5}$ atm and $>10^6$ at $pO_2 = 10^{-6}$–10^{-10} atm.

Introduction

The most important industrial use of gold and silver is in electrical and electronic equipment (EEE). Their quantities in electronics vary widely depending on the e-product and also through time and location [1]. In much of today's sophisticated electronic equipment, including cell phones, computers and televisions, the precious metal amounts are considerable, even up to several thousands of ppm [2]. Thus, Waste Electrical and Electronic Equipment (WEEE) can be considered a high-potential resource for gold and silver. The recoveries of gold and silver from WEEE are favorably performed in the current copper-making circuits including copper converters and secondary copper smelters such as the Ausmelt furnace [1, 3].

The research concentrating on minor element behavior in WEEE smelting is a relatively new field of science, and no experimental study has been performed to investigate gold and silver distributions between copper and alumina-saturated SiO_2-FeO_x-Al_2O_3 slags. The presence of alumina refers to scrap-copper ie. copper raffinate, which contains significant amounts of aluminum after mechanical separation [4, 5]. Overall, the literature concerning silver and gold behavior in slags is surprisingly scarce and lacks an agreement in solubility and in the dissolution mechanisms. Silver distribution in the copper matte-slag system has been investigated recently with ambiguous results [6-10]. However, silver equilibria in copper-slag systems have been

examined only in few experimental studies [10-13] and thermodynamic assessments (also Au) [14-16] despite numerous silver solubility studies in basic binary slags [17-21]. Gold equilibria in matte-slag system have been also explored by us [6, 7] and Yamaguchi *et al.* [22, 23]. Results from previous studies suggest that gold solubility in iron-silicate slag is effectively zero [24-27], and this idea has been used to detect mechanical copper or copper matte entrainment in slag. Interestingly, these studies reported gold concentrations of 40-80 ppm [25], 80 ppm [24] and 0-800 ppm (50-400 ppm for most of the data points) [26] in slags. Additionally, only few other experimental studies about gold solubility in slags have been performed [12, 28, 29].

The purpose of the present study is to investigate the distribution behavior of gold and silver between molten copper and alumina-saturated iron-silicate slag in the partial pressure range of $pO_2 = 10^{-5}$–10^{-10} atm at t = 1300 °C. The initial alumina concentration in the slag was set to 20 wt% in order to simulate the presence of aluminum in WEEE.

Experimental Procedure

Sample preparation

The copper master alloy was prepared by melting copper cathode (Boliden Harjavalta, 99.999 %) with approximately 1 wt% of Ag (Alfa Aesar, 99.95 %) and Au (Alfa Aesar, 99.95 %) in an alumina crucible. The melting was performed at 1400 °C under 99 % Ar – 1 % H_2 gas atmosphere for 12 hours. The master alloy was analyzed by EPMA. The initial gold content was measured to be 0.58 ± 0.13 wt% and silver 0.72 ± 0.21 wt%.

The slag mixture was prepared from pure commercial powders of Fe_2O_3 (Alfa Aesar, 99.99 %), SiO_2 (Umicore, 99.99 %) and Al_2O_3 (Sigma-Aldrich, 99.99 %). The components were weighed out to an initial composition of 52 % of Fe_2O_3, 28 % of SiO_2 and 20% of Al_2O_3. The slag components were thoroughly ground and mixed in agate mortar to form a homogeneous slag powder blend.

Experimental apparatus and method

The equilibration experiments were performed in a vertical tube furnace (Lenton LTF 16/45/450) including silicon carbide heating elements and an alumina reaction tube (impervious recrystallized alumina, 45 mm OD and 38 mm ID). The controller unit of the furnace was a Eurotherm 3216 PID. The furnace temperature was measured with a calibrated S-type Pt / 90 % Pt – 10 % Rh thermocouple (Johnson-Matthey, UK, accuracy ±3 °C) and the ambient room temperature with a Pt100 sensor (Platinum Resistance Thermometer; SKS Group, Finland). The Pt100 sensor and the S-type thermocouple were connected to a Keithley 2000 and 2010 multimeter – data loggers and the temperature measurement data were collected employing a NI LabVIEW temperature logging program. The experimental apparatus is illustrated schematically in Figure 1.

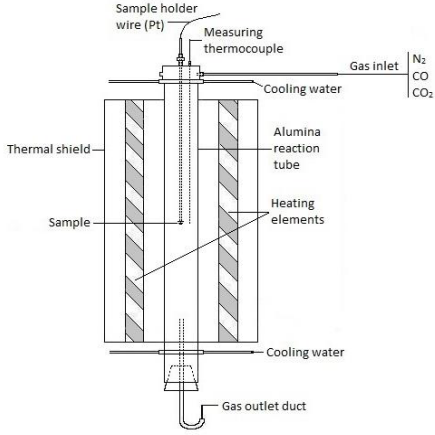

Figure 1. The experimental apparatus.

Three gases were connected to the inlet gas train: N_2 (purity ≥ 99.99 %), CO 4.7 (purity ≥ 99.997 %) and CO_2 5.2 (purity ≥ 99.9992 %; all from AGA, Finland). N_2 were controlled by rotameter after each experiment as flushing gas, whereas the reagent gases of CO and CO_2 were controlled by mass-flow controllers (Aalborg DFC26, USA; accuracy ±1 % of full scale). CO-CO_2 mixtures were employed in order to control the oxygen partial pressure (pO_2) in the furnace at the experimental temperature (1300 °C). The equilibrium reaction considered for gas atmosphere is,

$$CO + 1/2O_2 = CO_2. \tag{1}$$

The equilibrium constant K for reaction (1) is,

$$K = \frac{p_{CO_2}}{p_{CO} * p_{O_2}^{0.5}}. \tag{2}$$

The CO_2/CO ratios to produce the required oxygen partial pressures at 1300 °C were calculated using a K value of 71985.23 [31] and $p_{O_2}^{0.5}$ of the target partial pressure. The calculated CO_2/CO ratios for each oxygen partial pressure are shown in Table I. The CO_2/CO ratio was set for a total gas flow of 300 ml/min.

Table I. Calculated CO_2/CO flow ratios at 1300 °C.

p_{O_2}(atm)	CO_2/CO ratio
$1x10^{-5}$	227.64
$1x10^{-6}$	71.99
$1x10^{-7}$	22.76
$1x10^{-8}$	7.20
$1x10^{-9}$	2.28
$1x10^{-10}$	0.72

The required experimental time was determined with a set of experiments 1 h, 2 h, 4 h, 8 h and 16 h. According to SEM-EDS results for the slag, aluminous spinels and copper on these test samples, equilibrium was reached in 8 h. However, to absolutely ensure full equilibrium, the run time for the experiments was set to 16 h. For each experiment, approximately 250 mg of copper master alloy and 250 mg of slag mixture were placed into an alumina crucible. Commercial alumina (Degussit AL23, >99.5 % Al_2O_3) crucibles with ID of 8mm, OD of 10mm and depth of 15mm supplied by Friatec NA, Germany were employed in the experiments. Two sets of experiments were executed. The alumina crucible was hooked to a platinum wire (0.5 mm diameter) in the bottom end of the reaction tube and introduced into the furnace. While the gas atmosphere was stabilized for 30–60 minutes, the sample was kept in the cold zone of the furnace, after which the sample was pulled into the hot zone of the furnace and equilibration initiated. As the equilibration time (16 h) was reached, the sample was released and quickly quenched in an ice-water mixture.

Specimen analysis

The specimens were prepared for microanalysis by cutting the sample into half, mounting the cross-sections in epoxy resin and employing traditional wet metallographic techniques to achieve polished sections. The analyses were performed with a Cameca SX100 EPMA with Wavelength Dispersive spectrometers (WDS) and an Excite193 nm ArF laser ablation system (Teledyne CETAC Technologies, Omaha, USA) with a Nu AttoM SC ICPMS (Nu Instruments Ltd., Wrexham, UK).

The EPMA analyses were performed on copper, slag and solid aluminous spinel. The EPMA analyzing conditions used were: accelerating voltage 20 kV and beam current 40 nA. The beam diameter varied depending on the analyzed phase, for copper 100 µm, for spinel 1 µm and for slag 10–100 µm. The average elemental detection limits obtained are presented in Table II. The detection limits were not sufficient to define the precious metal concentrations in slag and in aluminous spinels reliably.

Table II. Elemental detection limits of EPMA (ppm).

O	Si	Cu	Al	Fe	Ag	Au
1315	223	239	240	230	402	1753

LA-ICP-MS analyses was performed to detect gold and silver concentrations in slag. 11 analysis spots were taken from each sample. The laser was run at a pulse frequency of 10 Hz and a pulse energy of 4 mJ at 40 % attenuation to produce a energy flux of 2.99 J/cm^2 on the sample surface with a 40 µm spot size. Analyses were made using time resolved analysis (TRA), with each analysis consisting of 20 seconds of background measurement prior to switching the laser on for 60 seconds of signal measurement. Synthetic NIST SRM 612 glass (concentrations reported in Jochum *et al.* [32]) and ^{29}Si have been used, respectively, as external and internal standards for quantification along with the USGS reference glass BHVO-2G as an internal check on data quality. The measurements were performed over 12 elements (Mg, Al, Si, Ca, Fe, Co, Ni, Cu, Ag, Pt, Au, Pb) at low resolution ($\Delta M/M = 300$) using the fast scanning mode. Baseline reduction and quantification of the trace element data was performed using the Glitter software package (GEMOC Laser ICP-MS Total Trace Element Reduction; Macquarie University, Australia). The instrumental uncertainty of the LA-ICP-MS technique was ± 5–10 %.

Results and discussion

Compositions of copper and slag

The experimental results, as calculated averages with standard deviations (1σ) for copper alloy and slag, are presented in Table III and Table IV, respectively.

Table III. EPMA results (wt-%) for copper alloy phase.

sample no.	pO2 (atm)	Cu	Ag	Au	O
F7	10^{-5}	95.66±0.13	0.90±0.05	0.81±0.06	0.88±0.05
F19	10^{-5}	94.99±0.17	1.02±0.04	1.06±0.11	1.07±0.12
F8	10^{-6}	95.63±0.35	0.82±0.08	0.83±0.08	0.86±0.13
F25	10^{-6}	96.09±0.11	0.95±0.08	0.82±0.07	0.59±0.08
F3	10^{-7}	95.79±0.20	0.89±0.07	0.84±0.08	0.73±0.10
F21	10^{-7}	96.05±0.17	0.94±0.10	0.81±0.08	0.77±0.05
F9	10^{-8}	95.27±0.29	0.88±0.04	0.83±0.07	0.69±0.05
F26	10^{-8}	96.05±0.11	0.93±0.07	0.82±0.06	0.65±0.07
F10	10^{-9}	95.63±0.30	0.81±0.03	0.77±0.05	0.70±0.05
F27	10^{-9}	96.04±0.12	0.90±0.05	0.85±0.07	0.63±0.05
F11	10^{-10}	95.65±0.20	0.81±0.05	0.70±0.10	0.70±0.06
F18	10^{-10}	95.36±0.12	0.94±0.05	0.83±0.05	0.72±0.06

Table IV. Slag analysis; EPMA results for main elements and LA-ICP-MS results for silver and gold. The number in brackets $^{()}$ refers to the number of analysis spots in which gold was observed above the detection limit and used to calculate the averages.

Sample no.	pO2 (atm)	EPMA (wt%)					LA-ICP-MS (ppm)	
		O	Si	Cu	Al	Fe	Ag	Au
F7	10^{-5}	33.30±0.37	11.08±0.22	23.94±0.55	9.27±0.18	22.30±0.31	596.41±72.58	0.12±0.05
F19	10^{-5}	34.22±0.18	11.88±0.23	22.18±0.61	9.58±0.09	22.02±0.26	624.92±47.50	0.05±0.01
F8	10^{-6}	35.28±0.30	14.44±0.23	12.28±0.27	10.06±0.15	27.88±0.11	257.95±8.57	$0.0066^{(5)}$
F25	10^{-6}	37.19±0.53	15.26±0.43	10.14±0.50	9.64±0.21	27.70±0.35	269.25±31.92	$0.0069^{(5)}$
F3	10^{-7}	36.16±0.47	15.57±0.22	5.38±0.03	9.82±0.17	33.01±0.18	116.92±16.77	$0.0065^{(2)}$
F21	10^{-7}	37.91±0.44	15.72±0.10	5.02±0.13	10.50±0.07	30.80±0.28	116.91±10.69	$0.0075^{(4)}$
F9	10^{-8}	37.29±0.19	15.57±0.08	2.87±0.02	10.20±0.08	34.09±0.14	61.60±3.28	$0.0066^{(2)}$
F26	10^{-8}	38.62±0.22	15.07±0.12	2.52±0.05	9.51±0.08	34.22±0.14	44.11±6.34	$0.0094^{(2)}$
F10	10^{-9}	36.79±0.17	15.76±0.12	1.51±0.02	10.42±0.07	35.46±0.13	25.43±4.04	$0.0073^{(2)}$
F27	10^{-9}	37.10±0.17	16.21±0.07	1.42±0.01	10.47±0.06	34.73±0.16	24.49±0.67	$0.0051^{(2)}$
F11	10^{-10}	38.64±0.24	14.94±0.07	0.80±0.01	9.92±0.09	35.65±0.26	11.32±0.37	$0.0070^{(5)}$
F18	10^{-10}	39.39±0.11	15.28±0.08	0.70±0.03	9.79±0.12	34.78±0.12	12.24±0.22	n.d.$^{(0)}$

The concentrations of gold and silver in copper stayed constant as a function of oxygen partial pressure. Smaller amounts of silicon (0.01–0.5 wt%), iron (0.01–0.7 wt%) and aluminum (0.03–0.04 wt%) were also detected in the copper phase.

The slag composition is highly dependent on the oxygen partial pressure, as can be seen in Table IV. Gold solubility in slag was mainly below the detection limits. Only for the highest oxygen partial pressure was gold detected in all analysis spots within the detection limits of LA-ICP-MS method employed. In lower oxygen partial pressures, gold was detected at concentrations between 5 and 9 ppb, and the average concentrations were calculated from the observed values in 0–5 analysis spots (marked in brackets in Table IV). To be strictly statistically correct, gold should be marked as n.d. (not detected) for all samples but F7 and F19.

Distribution coefficients of precious metals between copper and slag

The distribution coefficients of precious metals Me between copper and slag phases was defined as:

$$L^{Cu/s}[Me] = \frac{[wt-\%Me]_{copper}}{(wt-\%Me)_{slag}}, \quad (3)$$

where Me refers to silver and gold. The ratio is determined from the EPMA and LA-ICP-MS analyses, see Tables III and IV. The uncertainties for the distribution coefficients were calculated from the equation:

$$\frac{\sigma L^{Cu/s}[Me]}{L^{Cu/s}[Me]} = \left(\frac{\sigma}{\bar{x}}\right)_{slag} + \left[\frac{\sigma}{\bar{x}}\right]_{copper}, \quad (4)$$

where σ and $\bar{x}$ are the standard deviations and the (arithmetic) averages of Me respectively in slag () and copper [] phases.

The obtained distribution coefficients of silver with uncertainties as a function of oxygen partial pressure is presented in Figure 2. The (logarithmic) distribution coefficients increase linearly along with decreasing oxygen partial pressure with slope of 1/3.

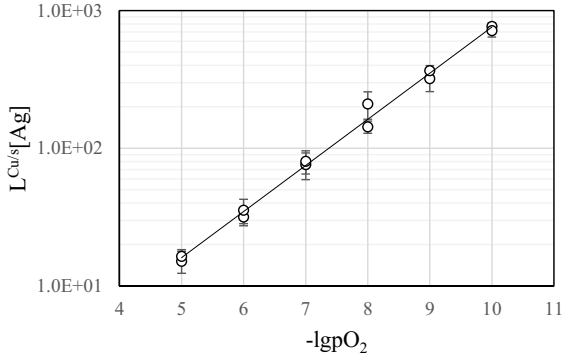

Figure 2. Distribution coefficients of silver between copper and FeO_x-SiO_2-Al_2O_3 slag at 1300 °C at a range of pO_2.

The observed solubility of gold in the slag was mainly below the elemental detection limit of out LA-ICP-MS method employed, being above the detection limit only in the highest pO_2 experiments. Figure 3 presents the distribution coefficient of gold between copper and slag as a function of oxygen partial pressure. The distribution coefficient of the detection limit (solid trend line) was calculated using the LA-ICP-MS detection limits of gold for the slag in the current measurements.

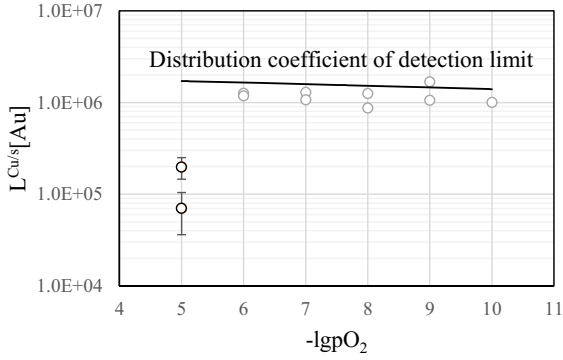

Figure 3. Distribution coefficients of gold between copper and FeO_x-SiO_2-Al_2O_3 slag at 1300 °C at a range of pO_2.

The distribution coefficients of gold in the pO2 range 10^{-6} to 10^{-10} are not reliable as they are calculated only from 2-5 analysis spot results. So, in reality the true distribution coefficients are greater than the distribution coefficient of the detection limit in the pO_2 range 10^{-6}–10^{-10} atm, and hence, these values can be used as the minimum distribution coefficients of gold in this partial pressure range. It can be concluded that in $pO_2 = 10^{-5}$ atm the distribution coefficient for gold is around 10^5 and in the pO_2 range 10^{-6}–10^{-10} atm, it is above 10^6.

The distribution equilibria of minor element Me between metal and slag can be presented with the following equation [16, 19, 33]:

$$[Me] + n/2O_2(g) = (MeO_n). \quad (5)$$

If the compositions of the phases and the activity coefficients of the species do not vary significantly, then equation (5) can be rewritten as:

$$Lg\ L^{Cu/s}[Me] = n/2lg\ pO_2 + lg\ C, \quad (6)$$

where C includes the activity coefficients, the equilibrium constant of equation (5) and the total number of moles in slag and copper. This thermodynamic approach can be used to define the oxidation state of the minor element in the slag. For silver, the slope of 1/3 (Figure 2) suggests a silver oxide form Ag3O2. However, there is no known silver oxide of this form, so possibly silver exists in the slag as a combination of different Ag species. Most previous studies have suggested Ag^+ ions ($AgO_{0.5}$) [10, 13, 18, 19] and Ag^0 [11, 30] in slag. However, although Takeda [10]

suggested Ag^+ ions to be present in slags, some of his slopes were close to 1/3 as in our study. In general, the distribution coefficient of silver in our study for alumina-saturated iron-silicate slags was higher than in Takeda's study [10] for all investigated slags.

Without any proper dependency between the distribution coefficient of gold and oxygen partial pressure, gold can be considered to dissolve into the slag as metallic species (Au^0). In Swinbourne's research [28] a combination of several Au species in IS and CF slags were suggested. In general, all the previous experimental studies [19, 24-26, 28, 29] show a higher gold solubility in the slags. In Celmer's study [34] of gold distribution in nickel matte-slag system, $L^{m/s}[Au]$, a significant difference between alumina-saturated and silica-saturated iron-silicate slag was found. At high matte grade (70 % Ni) the $L^{m/s}[Au]$ was 6x higher in alumina-saturation compared to silica-saturation. The solubility, dissolution mechanism and form of precious metals in slag are dependent on the oxygen pressure, temperature, the equilibrium system and the slag composition, especially basicity [20, 28]. Thus, as no previous studies in this system at these conditions exist, information drawn from the previous studies should be considered relevant but not directly analogous and comparable to the results presented here.

Conclusions

With only limited information presently available on the precious metal behavior in copper-slag systems, this investigation provides valuable new insights and results in the field of WEEE smelting and the copper manufacturing technologies. The equilibrium distributions of gold and silver between copper and alumina-saturated FeO_x-SiO_2-Al_2O_3 slag were determined in the oxygen partial pressure range 10^{-5}–10^{-10} atm at 1300 °C. An advanced and very sensitive experimental method, equilibration-quenching-EPMA/LA-ICP-MS, was applied in this study. The silver distribution coefficient increased exponentially from 30 to 1000 as a function of decreasing oxygen partial pressure. The gold distribution $L^{Cu/s}[Au]$ is 10^5 at $pO_2 = 10^{-5}$ atm and 10^6 at a minimum for $pO_2 = 10^{-6}$–10^{-10} atm. Further work, with higher doping levels and improved measurement parameters, should allow better definition of gold distribution at low pO_2 in these systems.

Acknowledgements

This research was financially supported by CLEEN Oy (Click Innovations OY), Kuusakoski Oy and Outotec as a part of ARVI project. The assistance of Lassi Pakkanen (GTK) in the EPMA analyses and Lassi Klemettinen in the LA-ICP-MS analyses is greatly appreciated.

References

[1] J. Cui, L. Zhang, *Journal of Hazardous Materials*, 158 (2008), 228-256.

[2] P. Chancerel, *Journal of Industrial Ecology,* 13 (2009), 791-810.

[3] M.E. Schlesinger *et al.*, *Extractive Metallurgy of Copper* (5th edition, Oxford UK: Elsevier, 2011), 455.

[4] M. Pizzol, M.S. Andersen, M. Thomsen, "Greening of Electronics" (Danish Ministry of the Environment, Environmental, Project No. 1416, 2012).

[5] G. John *et al.*, "MTDATA and the Prediction of Phase Equilibria in Oxide Systems: Thirty Years of Industrial Collaboration", Submitted to *Metallurgical and Materials Transactions B*, 2016.

[6] K. Avarmaa *et al.*, *Journal of Sustainable Metallurgy*, 1 (2015), 216-228.

[7] K. Avarmaa, H. Johto, P. Taskinen, *Metallurgical and Materials Transactions B*, 47 (2014), 244-255.

[8] G. Roghani, Y. Takeda, K. Itagaki, *Metallurgical and Materials Transactions B,* 31 (2000), 705-712.

[9] G. Roghani, M. Hino, K. Itagaki, "Phase Equilibrium and Minor Element Distribution between Slag And Copper Matte under High Partial Pressures of SO_2", (Paper presented at the International Conference on Molten Slags, Fluxes and Salts, 1997), 693-703.

[10] Y. Takeda, G. Roghani, "Distribution Equilibrium of Silver in Copper Smelting System", (Paper presented at the first International Conference on Processing Materials for Properties: Honolulu, USA, 7-10 Nov., 1993), 357-360.

[11] F. Richardson, J. Billington, *Bull. Institution of Mining and Metallurgy,* 593 (1956), 273-297.

[12] P. Mackey, G. McKerrow, P. Tarassoff, "Minor Elements in the Noranda Process", (Paper presented at the 104th AIME Annual Meeting, New York, 1975), 27.

[13] Y. Takeda, *Transactions of the Japan Institute of Metals,* 24 (1983), 518-528.

[14] M. Nagamori, P. Mackey, *Metallurgical Transactions B*, 9 (1978), 567-579.

[15] K. Nakajima *et al.*, *Environmental Science and Technology*, 45 (2011), 4929-4936.

[16] K. Nakajima *et al.*, *Materials Transactions*, 50 (2009), 453-460.

[17] J.H. Park, D.J. Min, *Metallurgical and Materials Transactions B* 30 (1999), 689-694.

[18] J.H. Park, D.J. Min, *Materials Transactions*, JIM, 41 (2000), 425-428.

[19] D. Swinbourne, "Solubility of Precious Metals in Slags", (Paper presented at the European Metallurgical Conference, EMC 2005), 1, 223-235.

[20] D. Swinbourne, X. You, *Transactions of the Institution of Mining and Metallurgy Section C-Mineral Processing and Extractive Metallurgy*, 108 (1999), C59-C65.

[21] B. ZIOŁEK, W. Szklarski, A. Bogacz, *Archives of metallurgy*, 36 (1991), 395-408.

[22] H.M. Henao, K. Yamaguchi, S. Ueda, "Distribution of Precious Metals (Au, Pt, Pd, Rh and Ru) between Copper Matte and Iron-Silicate Slag at 1573 K", (Paper presented at the TMS Fall Extraction and Processing Division: Sohn International Symposium, San Diego, USA, 27-31 August 2006), 1, 723-729.

[23] K. Yamaguchi, "Distribution of Precious Metals between Matte and Slag and Precious Metal Solubility in Slag", (Paper presented at the Copper 2010), 3, 1287-1295.

[24] R. Altman, *Transactions of the Institution of Mining and Metallurgy*, 81 (1972), 163-175.

[25] J. Taylor, J. Jeffes, *Transactions of the Institution of Mining and Metallurgy Section C-Mineral Processing and Extractive Metallurgy*, 84 (1975), C18-24.

[26] J.M. Toguri, N.H. Santander, *Metallurgical Transactions*, 3 (1972), 586-588.

[27] A. Geveci, T. Rosenqvist, *Transactions of the Institution of Mining and Metallurgy*, 82 (1973), 193-201.

[28] D. Swinbourne, S. Yan, S. Salim, *Mineral Processing and Extractive Metallurgy*. 114 (2005), 23-29.

[29] Y.S. Han, D.R. Swinbourne, J.H. Park, *Metallurgical and Materials Transactions B*, 46 (2015), 2449-2457.

[30] M. Kashima, M. Eguchi, A. Yazawa, *Transactions of the Japan Institute of Metals,* 19 (1978), 152-158.

[31] A. Roine, HSC Chemistry for Windows, vers. 6.12, Outotec Research, Pori. 2007.

[32] K.P. Jochum *et al.*, *Geostandards and Geoanalytical Research,* 35 (2011), 397-429.

[33] A. Yazawa, "Thermodynamic Interpretation on Oxidic Dissolution of Metal in Slag", (Paper presented at the Pyrometall. Complex Mater. Wastes, Aust. Asian Pac. Course Conf. Minerals, Metals and Material Society, Warrendale, 1994), 61-72.

[34] R.S. Celmer, "Cobalt and Gold Distribution in Nickel-Copper Matte Smelting", (Paper presented at the Nickel Metallurgy, Symposium Proceedings 25th Annual Conference Metallurgy, Toronto, Canada 17-20 August 1986), 1, 147-163.